European Conference on Optical Communication (ECOC) 2022 © Optica Publishing Group 2022

Beam-curvature-compensated Solid-state Beam Scanner Integrated with Multi-grating Pitch Tunable Slow-light VCSELs for Enhanced Field of View

Ruixiao Li(1), Xiaodong Gu(1,2), Satoshi Shinada(3), Fumio Koyama(1)

(1) Institute of Innovative Research (IIR), Tokyo Institute of Technology, 4259-R2 Nagatsuta, Yokohama, 226-8503 Japan, li.r.ae@m.titech.ac.jp
(2) Ambition Photonics Inc., Tokyo Tech Yokohama Venture Plaza E208, Yokohama, 226-8510 Japan
(3) National Institute of Information and Communications Technology, Japan

Abstract *We realized 1D solid-state VCSEL beam scanner with field of view (FOV) of >24°×15° integrating tunable VCSELs of different surface grating pitches. We also compensated the curvature of output fan beam by introducing curved prism mirror. The FOV was expanded to > 64°×14° with DOE.*

Introduction

Nowadays, 3D sensing are welcoming the market blowout thanks to its applications in LiDARs for automotive and robots, time-of-flight camera for mobile phones. For next-generation solid-state 3D sensing, a high-resolution beam scanner has been attracting more attention. Being a mature technology, beam scanners using mechanical and MEMS technology has been applied in current 3D sensors [1], but its inserted movable element brings concerns about its long-term reliability, module size and cost efficiency. Therefore, non-mechanical beam scanning technology, such as optical phased array [2] and modulated photonic crystal laser [3] offer a new opportunity for 3D sensing. However, their limited resolution, small field of view (FoV) and hard integrability with a light source are still challengeable for practical applications.

In recent years, a beam scanner based on VCSEL was invented, which could realize beam scanning with FoV of >10° and resolution of >200 without requirement of an external light source [4]. Assisted with diffractive optical element (DOE), FoV of >100° and a record high resolution of > 1400 was relized [5]. However, using of DOE leads to power penalty due to beam splitting, which makes it difficult for application in long-range LiDARs. Besides, the curvature of beam scanner leaves concern about cooperation with an area-scan time-of-flight (ToF) camera, which has higher shutter speed and better signal to noise ratio than global-shutter exposure camera. In this paper, we firstly proposed a VCSEL beam scanner integrated to multi-pitch tunable slow-light VCSELs to enhance the FoV without using DOE. Then, we proposed a novel curved prism mirror to compensate the curvature of output beam. The FOV could also be expanded over 64°×14° thanks to DOE.

Enhanced-FoV beam steering by integrating multi-pitch surface grating tunable VCSELs

Figure 1 (a) illustrates the basic schematic of our VCSEL beam scanner. It is composed of a VCSEL beam scanner shared by two integrated tunable surface grating slow-light VCSELs [6]. The scanner was based on a high-dispersion VCSEL waveguide. It could steer the output angle θ_{out} with tuning the lasing wavelength of slow-light VCSELs λ_{in} as shown by Eq. 1 [7],

$$sin\theta_{out} = n_{wg}\sqrt{1-(\frac{\lambda_{in}}{\lambda_{cutoff}})^2} \qquad (1)$$

where n_{wg} and λ_{cutoff} is the refractive index and cutoff wavelength of a VCSEL waveguide, respectively. Because the tunable surface grating

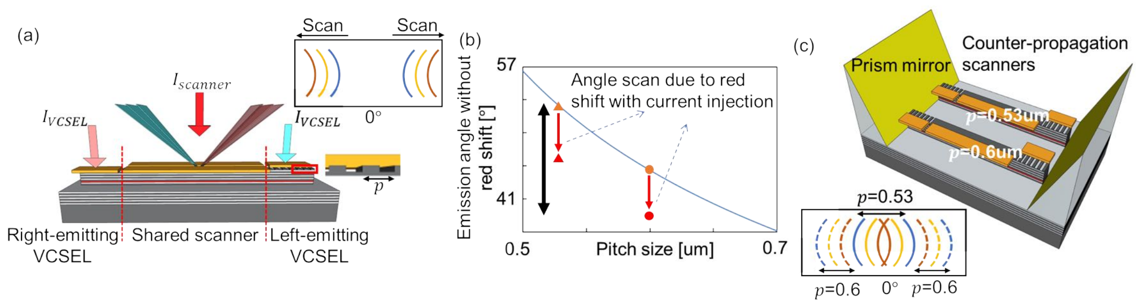

Fig. 1: (a) Schematic of electrical-driven counter-propagation-switchable beam scanner; (b) Relation between pitch size of grating on slow-light VCSEL and principle of enhancing FoV by multi-pitch beam scanner (c) Schematic of measuring FFP of proposed multi-pitch beam scanners

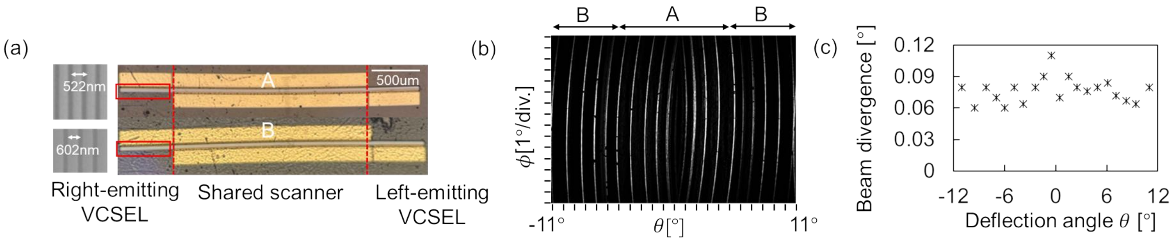

Fig. 2: (a)Photo of beam scanner with two kinds of pitch size (b) FFP of out beam reflected by the prism mirror (c) Beam divergence of beams

slow-light VCSELs were integrated at two sides of the scanner, the light could be emitted in counter direction by switching two VCSELs. The scanner also works as an amplifier with amplification of >30dB by injecting $I_{scanner}$ of >5A. The lasing wavelength of tunable slow-light VCSELs was determined by the pitch p of grating loaded on the VCSEL [6]. Therefore, the correspondence of pitch and output angle without considering thermal-effected red shift could be found in Fig. 1 (b). The orange markers show two examples when p is 530nm and 600nm. With tuning the current injected into VCSELs I_{VCSEL}, the output angle will steer thanks to the red shift of VCSELs as shown in the red arrows and markers in Fig. 1 (b). However, the scanning range limited to <10° due to thermal effect for a single device. If two devices with different pitches were integrated as shown in Fig.1 (c), the scanning range could be double as bold arrows in Fig. 1 (b). The prism mirror was placed beside the scanner to make output beam cover 0°. It could be estimated that if scanners with more kinds of grating pitch are integrated, the scanning range could be further improved unless the lasing wavelength are too far away from the gain-peak wavelength.

Two beam scanners with pitch size of about 520nm (Scanner A) and 600nm (Scanner B) were integrated as shown in Fig.2 (a). The length of scanner and tunable slow-light VCSEL are 2mm and 0.5mm respectively. By tuning the I_{VCSEL} from 60-272mA for scanner A and injecting $I_{scanner}$ of 208mA, the output beam covers the FoV from -6° to 6° as shown in the middle part in Fig.2 (b). Similarly, by tuning the I_{VCSEL} from 50-245mA for scanner A and injecting $I_{scanner}$ of 190mA to scanner B, it could be found that the far field pattern (FFP) of output beam shown in Fig. 2 (b) covers from -11° to -6° and -6° to 11°. In total, FoV of 24° ×15° was obtained. The beam divergence was also measured in Fig. b (c). The average beam divergence is 0.076°. It indicates the total resolution number of 315 for the integrated chip. By better fabrication process, better beam divergence of <0.06° could also be expected. By integrating another beam scanner with pitch size of 660nm, the FoV could be further increased to 28°. We could also expect the FoV of >100° by using a 3-spot DOE, which provides much larger beam intensity than our previous result [5].

Beam curvature compensation by adding a curved prism mirror

From Fig. 2 (b), it could be seen that the original output beam has curvature. It leads to difficulty in being received by an area-scan ToF camera, because shutter shape of most area-scan is a line (for example, 2 pixels × 600 pixels). An area-scan camera is a very promising receiver for long-range LiDARs, because it has higher shutter speed and better signal to noise ratio compared to the conventional global-shutter ToF camera by avoiding the effect of background sublight. Therefore, it is significantly meaningful to compensate the beam curvature. To estimate the beam curvature, we defined maximum deflection angle difference of single beam $\Delta\theta$ as shown in Fig. 3 (a). When the $\Delta\theta$ is large, it needs more pixels to receive the beam for the area-scan

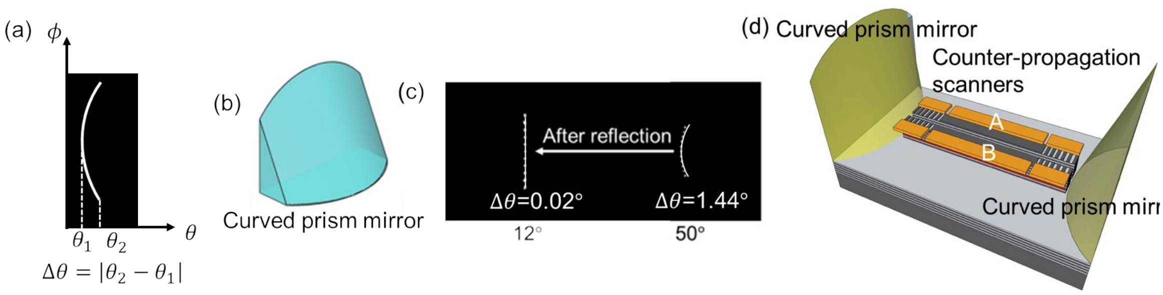

Fig. 3: Scanned FFP of counter-propagation beam scanner with curved prism mirrors

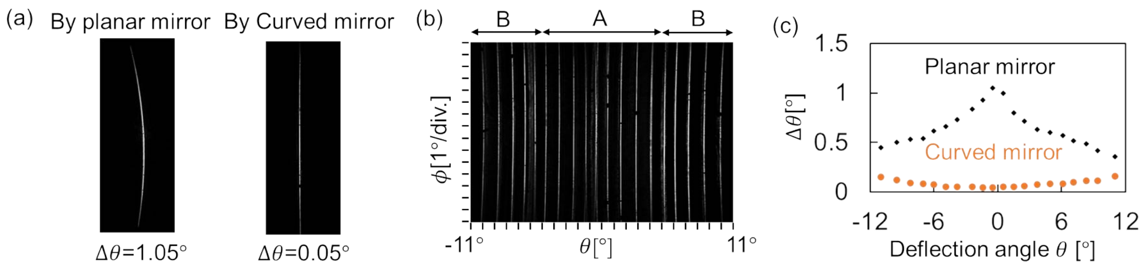

Fig. 4: (a) Comparison of beam reflected by planar and curved prism mirror (b) curvature-compensated beam steering FFP (c) Comparison of $\Delta\theta$ reflected by planar and curved prism mirror

camera, which will reduce the shutter speed and signal to noise ratio. To compensate the curvature, a concave prism mirror shown in Fig. 3 (b) was proposed and fabricated. Differing from a planar prism mirror, the output angle after reflection will be modulated by the incident angle. It enables us to obtain a straight line beam even if the incident beam has curvature. The curved prism mirror was designed and simulated in Zemax, which gave the simulation performance as shown in Fig. 3 (c). When a beam with $\Delta\theta$ of 1.44° and deflection angle of 50° incidents to the prism, the $\Delta\theta$ will be compensated and the beam divergence in the ϕ direction will be expanded. Like the last section, we could replace the planar prism mirror by the curved prism mirror and get the beam scanning with the same FoV and less curvature as shown in Fig. 3 (d). Because the curvature compensation performance is very sensitive to the relative position of beam scanner and prism mirror, the two scanners (scanner A and B) was arranged very closed (scanner space is 50μm) and symmetrical to the prism mirror.

The experimental result was shown in Fig. 4. Fig. 4 (a) shows the comparison of beams reflected by the planar and curved prism mirror when the I_{VCSEL} is 60mA for right-emitting scanner of scanner A. It could be seen that $\Delta\theta$ was significantly reduced from >1° to 0.05°, which meets the requirement for most of area-scan cameras. Because the beam curvature varies with deflection angle changing, the curvature compensation of whole scanning range was also illustrated in Fig. 4 (b). The obvious curvature improvement could be witnessed in the entire scanning range. The $\Delta\theta$ was also measured as shown in Fig. 4 (c). The average $\Delta\theta$ was reduced from 0.648° to 0.084° by introducing the curved prism mirror. However, the performance degradation could be observed when the deflection angle goes away from 0°, because of the beam curvature variation.

The FoV could be easily expanded by putting a 1D DOE as shown in Fig. 5(a). We used a counter-propagation single-grating-pitch beam scanner with curved prism mirrors and 10-spot 1D DOE. It covers the FoV of >64° with the number of resolutions points over 810. The average $\Delta\theta$ was improved from 1° to <0.08° thanks to the curved prism mirror.

Conclusions

We proposed and demonstrated a counter-propagation-switchable beam scanner by integrating two tunable slow-light VCSELs. By integrating tunable VCSELs with two different surface grating pitches, the beam scanning range was increased double, which could be further improved by integrating more scanners with different pitches. We also compensated the beam curvature from $\Delta\theta$ =0.648 ° to $\Delta\theta$ =0.084 ° by introducing a curved prism mirror. It makes the beam scanner more applicable for 3D sensing, especially long-range LiDARs with area-scan ToF sensors.

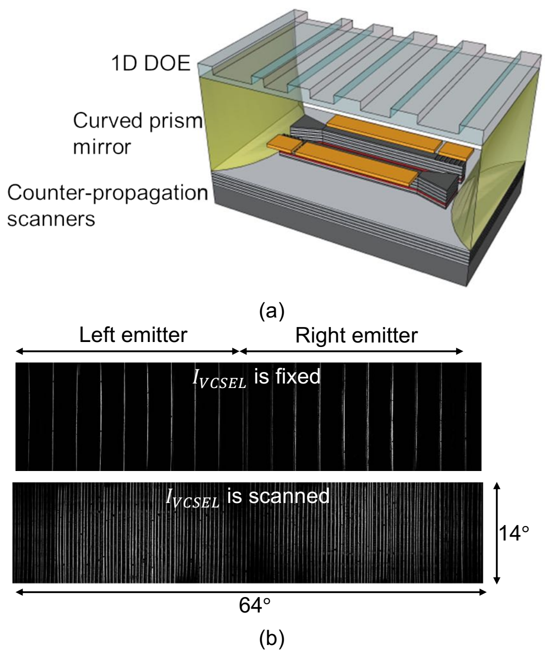

Fig. 5: (a) Counter-propagation single-grating-pitch beam scanner with curved prism mirrors and DOE, (b) Scanning FFPs with beam curvature compensation

Acknowledgements

This work was supported by Japan Science and Technology Agency (#JPMJTR211A).

References

[1] S. T. S. Holmström, U. Baran, and H. Urey, “MEMS laser scanners: A review,” *J. Microelectromechanical Syst.*, vol. 23, no. 2, pp. 259–275,2014, doi: 10.1109/JMEMS.2013.2295470.

[2] J. Sun, E. Timurdogan, A. Yaacobi, E. S. Hosseini, and M. R. Watts, “Large-scale nanophotonic phased array,” *Nature*, vol. 493, no. 7431, pp. 195–199, 2013, doi: 10.1038/nature11727.

[3] R. Sakata *et al.*, “Dually modulated photonic crystals enabling high-power high-beam-quality two-dimensional beam scanning lasers,” *Nat. Commun.*, vol. 11, no. 1, pp. 1–10, 2020, doi: 10.1038/s41467-020-17092-w.

[4] S. Hu, X. Gu, A. Hassan, R. Li, M. Nakahama, S. Shinada, and F. Koyama, “Ultra-compact VCSEL scanner for high power solid-state beam steering,” Optics Express, vol. 30, no. 6 pp. 8742-8749, 2022 doi: 10.1364/OE.453090.

[5] R. Li, S. Hu, X. Gu, and F. Koyama, “Compact solid-state vertical-cavity-surface-emitting-laser beam scanning module with ultra-large field of view,” *Appl. Phys. Express*, vol. 14, no. 11, p. 112005, 2021, doi: 10.35848/1882-0786/ac2ff8.

[6] A. M. A. Hassan, X. Gu, M. Nakahama, S. Shinada, M. Ahmed, and F. Koyama, “High-power operations of single-mode surface grating long oxide aperture VCSELs,” *Appl. Phys. Lett.*, vol. 119, no. 19, p. 191103, 2021, doi: 10.1063/5.0066590.

[7] X. Gu, T. Shimada, A. Matsutani, and F. Koyama, “Miniature nonmechanical beam deflector based on bragg reflector waveguide with a number of resolution points larger than 1000,” IEEE Photonics J. vol. 4, no.5, pp.1712–1719, 2012, doi: 10.1109/JPHOT.2012.2214206.